Appl Microbiol Biotechnol (2012) 95:1021–1034
DOI 10.1007/s00253-012-3938-y

Comparison of the transient responses of *Escherichia coli* to a glucose pulse of various intensities

Sirichai Sunya · Frank Delvigne · Jean-Louis Uribelarrea · Carole Molina-Jouve · Nathalie Gorret

Received: 22 December 2011 / Revised: 1 February 2012 / Accepted: 1 February 2012 / Published online: 29 February 2012

Abstract Dynamic stimulus-responses of *Escherichia coli* DPD2085, *yciG::LuxCDABE* reporter strain, to glucose pulses of different intensities (0.08, 0.4 and 1 gL^{-1}) were compared using glucose-limited chemostat cultures at dilution rate close to 0.15 h^{-1}. After at least five residence times, the steady-state cultures were disturbed by a pulse of glucose, engendering conditions of glucose excess with concomitant oxygen limitation. In all conditions, glucose consumption, acetate and formate accumulations followed a linear relationship with time. The resulting specific uptake and production rates as well as respiratory rates were rapidly increased within the first seconds, which revealed a high ability of *E. coli* strain to modulate its metabolism to a new environment. For transition from glucose-excess to glucose-limited conditions, the cells rapidly re-established its pseudo-steady state. The dynamics of transient responses at the macroscopic viewpoint were shown to be independent on the glucose pulse intensity in the tested range. On the contrary, the *E. coli* biosensor *yciG::luxCDABE* revealed a transcriptional induction of *yciG* gene promoter depending on the quantities of the glucose added, through in situ and online monitoring of the bioluminescence emitted by the cells. Despite many studies describing the dynamics of the transient response of *E. coli* to glucose perturbations, it is the first time that a direct comparison is reported, using the same experimental design (strain, medium and experimental set up), to study the impact of the glucose pulse intensity on the dynamics of microbial behaviour regarding growth, respiration and metabolite productions.

Keywords Dynamic responses · *Escherichia coli* biosensor *yciG::luxCDABE* · Effect of the glucose intensity · Glucose pulse · In situ and online bioluminescence monitoring

Electronic supplementary material The online version of this article (doi:10.1007/s00253-012-3938-y) contains supplementary material, which is available to authorized users.

S. Sunya · J.-L. Uribelarrea · C. Molina-Jouve · N. Gorret (✉)
Université de Toulouse; INSA, UPS, INP, LISBP,
135 Avenue de Rangueil,
31077 Toulouse, France
e-mail: nathalie.gorret@insa-toulouse.fr

S. Sunya · J.-L. Uribelarrea · C. Molina-Jouve · N. Gorret
INRA, UMR792,
31400 Toulouse, France

S. Sunya · J.-L. Uribelarrea · C. Molina-Jouve · N. Gorret
CNRS, UMR5504,
31400 Toulouse, France

F. Delvigne
University of Liège, Gembloux Agro-Bio Tech,
Unité de Bio-industries/CWBI,
Passage des Déportés 2,
5030 Gembloux, Belgium

Introduction

With the increasing interest in the use of bioprocesses to substitute traditional chemical processes for production of synthons (chemical intermediates, building blocks etc.) and/or biomolecules (metabolites, recombinant proteins etc.), a deep understanding of the dynamics of interactions between microorganism and microenvironment is one of the major challenges to improve the bioprocess scale-up (Neubauer and Junne 2010). Indeed, it is well-known that inside industrial bioreactors microorganisms encounter local concentration gradients, due to both process mode and mixing efficiency which affect the global bioprocess performance (Enfors et al. 2001; Hewitt et al. 2007; Lara et al. 2006a;

Nienow 2009). Many industrial biotechnologies usually use fed-batch mode where a high concentration of feed substrate is added at one point on the top of the large-scale bioreactor leading to local glucose gradients (Enfors et al. 2001). Microorganisms circulating inside the different zones of the large-scale bioreactor are in fact submitted to various kinds of microenvironment perturbations which could affect the microorganism physiology: induction of stress responses, metabolic shifts for example (Lara et al. 2006a). In the case of *Escherichia coli*, a high concentration of glucose would induce the well-known acetate overflow mechanism with a concomitant local acidification (Eiteman and Altman 2006; Lara et al. 2008; Neubauer et al. 1995; Wolfe 2005). This glucose excess could moreover lead to a local oxygen limitation which could engender the fermentation metabolic pathways (Clark 1989; Xu et al. 1999), thereby organic acid accumulation.

Up to now, several studies investigating the effect of substrate gradients on *E. coli* responses were conducted both in large-scale bioreactors (Bylund et al. 1998; Enfors et al. 2001; Xu et al. 1999) and in scale-down bioreactors using different operating culture modes: fed batch (Hewitt et al. 2000; Lin et al. 2001; Lin and Neubauer 2000; Xu et al. 1999) or chemostat (Buchholz et al. 2002; Chassagnole et al. 2002; De Mey et al. 2010; Hoque et al. 2011; Hoque et al. 2005; Lara et al. 2009; Schaefer et al. 1999; Schaub and Reuss 2008; Taymaz-Nikerel et al. 2011). In order to simulate substrate gradients occurring in large-scale bioreactors, the scale-down strategy involved one- or two-stage systems: one-stage system using substrate-limited chemostat culture with pulse type perturbation (Taymaz-Nikerel et al. 2011; Theobald et al. 1993); two-stage systems consisting of a stirred-tank reactor combined with a plug-flow reactor (PFR) with circulation loop between the two compartments (Buchholz et al. 2002; Buziol et al. 2002; Lara et al. 2009; Visser et al. 2004). However, the limits of the latter system are linked to the difficulties to get a direct measurement of oxygen concentrations created by substrate gradients and to sample along the PFR. Furthermore, the circulation time and the volume ratio between the two compartments led to different competence states of the strain related to the history of the cells, thus the resulting behaviour to the stress conditions corresponds to the behaviour of different population classes.

In order to investigate and compare the effect of a single perturbation on the cell behaviour, substrat-limited chemostat culture is a precious tool to maintain cells in a chosen physiological steady state. Most of the studies using chemostat mode have been carried out at low dilution rate ($<0.2 h^{-1}$) to avoid co-metabolite productions, only biomass should be produced in those conditions. However, Schaub and Reuss (2008) studied the effect of glucose pulse on different dilution rates in order to quantify the impact on intracellular metabolite concentrations and thus to provide information on the dynamic behaviour of the superior part of the glycolytic pathway which is involved in the PTS transport. Different wild-type strains, gene knock-out mutants and different type of pulses were carried out and the resulting microbial responses were analysed at the macroscopic level (kinetics of substrate uptake and extracellular metabolite productions, intracellular metabolite quantifications, and metabolic flux analysis) (Buchholz et al. 2002; Chassagnole et al. 2002; De Mey et al. 2010; Hoque et al. 2011; Hoque et al. 2005; Lara et al. 2009; Schaefer et al. 1999; Schaub and Reuss 2008; Taymaz-Nikerel et al. 2011) and at the molecular level using microarrays and quantitative RT-PCR (Ishii et al. 2007; Lara et al. 2006b). Perturbations with different substrates (glucose, glycerol, pyruvate, succinate and acetate) were also conducted (Buchholz et al. 2002; Link et al. 2010).

Despite a growing number of studies describing the transient microbial responses to a sudden change of substrate concentration, it is still quite difficult to evaluate whether *E. coli* would have a similar behaviour in response to a glucose pulse of different intensities due to the various experimental designs: various strains, media, pulse intensities, analytical methods and sampling methods. In this context, the purposes of this paper are: (1) to present a direct comparison of the dynamics of the transient responses of *E. coli* DPD 2085, containing *yciG::luxCDABE* fusion, to a glucose pulse of three different intensities on steady-state glucose-limited chemostats under the same operating conditions; (2) to investigate the impact of the glucose pulse intensity on the transcriptional induction of a specific promoter which involved in stress response by means of the biosensor *E. coli* strain through in situ and on-line bioluminescence monitoring. However, this latter part has been specifically described in the previous work (Sunya et al. 2012), and this paper focuses on the integration of both the dynamics of extracellular metabolite response and the induction of the transcriptional response.

Materials and methods

Bacterial strain

The strain *E. coli* DPD2085 which is a plasmid-based *lux* fusion was obtained from DuPont Company (USA). Plasmid/strain construction has been previously described (Van Dyk et al. 1998; Van Dyk and Rosson 1998; Van Dyk et al. 2001b; Zanzotto et al. 2006). Briefly a plasmid pDEW215 was constructed from a moderate-copy-number probe vector pDEW201 containing the promoterless *luxCDABE* cassette from *Photorhabdus luminescens*. The probe vector construction and its restriction map were

described in detail by Van Dyk and co-workers (Van Dyk et al. 2001a; Van Dyk and Rosson 1998). The *yciG* gene promoter was fused to the probe vector pDEW201 in appropriate orientation to give a plasmid named pDEW215. Then the plasmid transformation, pDEW215, was introduced in *E. coli* strain DPD1675 used as the host strain for screening for induction of bioluminescence from the *yciG::luxCDABE* genetic fusion.

The strain was maintained at −80°C in Luria-Bertani (LB) medium (10 gL^{-1} tryptone, 10 gL^{-1} NaCl, 5 gL^{-1} yeast extract and 5 gL^{-1} glucose), supplemented with 75 mg L^{-1} ampicillin, 75 mg L^{-1} streptomycin and 30% (*v*/*v*) glycerol (glycerol stocks).

Minimum media composition

The defined minimum medium (MM) used for all batch and continuous fermentations was the following (all concentration in grammes per litre): $C_6H_8O_7$ (citric acid), 3.0; K_2HPO_4, 4.0; Na_2HPO_4 $12H_2O$, 1.0; $(NH_4)_2SO_4$, 0.375; $(NH_4)_2HPO_4$, 4.0; NH_4Cl, 0.065; $MgSO_4$ $7H_2O$, 0.5, $CaCl_2$. $2H_2O$, 0.02; $FeSO_4$; $7H_2O$, 0.02; thiamine-HCl, 0.01; $MnSO_4$ H_2O, 0.01; $CoCl_2$ $6H_2O$, 0.004; $ZnSO_4$ $7H_2O$, 0.002; Na_2MoO_4 $2H_2O$, 0.002; $CuCl_2$; $2H_2O$, 0.001; H_3BO_3, 0.0005, prepared in deionised water. The pH was adjusted to 6.7 by addition of 28% (*w*/*w*) ammonia solution prior to sterilisation. After sterilisation of the medium, 10 gL^{-1} glucose, 150 mg L^{-1} ampicillin and 0.5 mL L^{-1} polypropylene glycol (antifoam PPG) were added in the culture.

Batch and continuous cultures

Batch and continuous fermentations were carried out in a 1.6-L stainless-steel stirred tank bioreactor (11 cm diameter×20 cm total height) with a working volume of 1 L (BIOSTAT® Bplus, Sartorius, Germany). The vessel was equipped with 2 six-bladed Rushton impellers, fitted with four equally spaced baffles (1 cm width), with dissolved oxygen, pH, temperature probes, stirred speed and airflow controls. Regulation and monitoring were done using MFCS/win 2.1 software package.

For each culture, one glycerol stock was streaked on a Petri dish and incubated overnight at 37°C. Only one colony was used for the pre-culture. Three successive steps of precultures were then carried out in baffled-shake flasks at 10% (*v*/*v*) ratio with increasing culture volumes (5 mL LB, 5 mL MM and 100 mL MM). The flasks were incubated at 37°C overnight.

The 100 mL preculture was used for inoculating the bioreactor. Cells were exponentially grown in batch mode and subsequently, a glucose-limited continuous mode of operation was initiated by feeding fresh medium (MM supplemented with 10 gL^{-1} glucose and 10 mg L^{-1} thiamine) and removing broth from the bioreactor by means of a stainless steel cannula placed at the upper level of 1-L culture. The reactor was stirred at 800 rpm and aerated at 0.5 vvm to ensure a well-mixed reactor without any oxygen limitation. An overpressure of 60 mbars was applied in the bioreactor headspace. pH was maintained at 6.70 and regulated by addition of 7% (*v*/*v*) ammonia solution. The antifoam (PPG) and ampicillin were added to maintain their constant concentrations in the bioreactor. All continuous cultures were carried out at a dilution rate close to 0.15 h^{-1}. The system was considered to be in a steady state after at least five residence times.

Glucose pulse experiments and sampling system

A sugar pulse was performed into the bioreactor by a rapid injection of a sugar-concentrated solution using a sterile syringe through a septum placed on the top of the reactor. The volume injected was less than 0.5 % of the total working volume. During the course of the glucose pulse, the medium feed had kept running. Samples were taken before and after the glucose pulse. In this paper, three independent glucose pulses of different intensities (0.08, 0.4 and 1 gL^{-1}) were carried out on the characterised steady-state culture.

Samples for extracellular metabolite analysis were obtained by continuously withdrawing the broth from the bioreactor using a rapid sampling system. This vacuum filtration system is composed of a Multiscreen® HTS 96-well filter plate (0.45 μm pore size filter, Durapore® Membrane, Massachusetts, USA) and of a receiver plate (0.8 mL 96-well storage plate, Thermo Scientific, UK) combined with a vacuum pump. Direct withdrawal of the broth at the middle of the bioreactor was performed via a needle connected to sampling tubing at the rate of 175 μL s^{-1} with a small dead volume of 0.42 mL as well as a short residence time of 2 s. The broth was quasi-instantaneously filtered. Then the supernatant of about 30–50 μL was collected for each sample in the 96-well receiver plate which was then kept at −4°C for further extracellular metabolite analysis.

Chemical products

The purchased chemicals were of the highest grade commercially available. The salts except for magnesium sulphate (Panreac, France), oligo-elements, orthophosphoric acid and ammonia solution were provided by Rectapur/Normapur/Prolabo. Thiamine-HCl and ampicillin-Na were purchased from Sigma (USA). A 46/51% (*w*/*w*) sodium hydroxide solution was obtained from Fischer Scientific (UK). Glucose and fructose were obtained from Rectapur/Prolabo respectively and sucrose from Merck (Germany).

Biomass determination

Cell biomass was determined from optical density measurement at 620 nm (OD_{620nm}) using a visible spectrophotometer (Biochrom Libra S4) with a 2-mm absorption cell (Hellma). OD_{620nm} was calibrated against cell dry weight measurements. The cells were harvested by filtration on 0.20-μm-pore-size polyamide membranes (Sartorius Biolab Product) and dried in an oven at 60°C (with the presence of gel silica) under a vacuum of 200 mm Hg (~26.7 kPa) for at least 48 h (HERAEUS, France). One unit in OD_{620nm} value corresponded to 2.06 gL^{-1} biomass dry weight concentration during steady-state cultures.

Determination of plasmid stability

In order to verify that we were able to maintain a homogeneous population of our mutant *E. coli* strain throughout the chemostat runs, plasmid stability of the culture was assessed. The numbers of plasmid-bearing cells and of the total cells were determined using a simple plate count method on plate count agar (PCA) medium with and without antibiotic, respectively. Steady-state broth samples were withdrawn from the chemostat culture (about 8-h interval). One millilitre of broth was serially diluted with 9-mL sterile physiological solution of 0.85% NaCl (*w*/*v*; BioMerieux®, France) and 50 μL of the resulting cell suspension were plated out, in triplicate, onto PCA medium with and without 150 mg L^{-1}ampicillin by means of a Whitley Automatic Spiral Plater-WASP (Don Whitley Scientific Limited, UK). The plates were incubated overnight at 37°C, and the colonies were manually counted. Percentage of the ratio between plasmid-bearing colonies and total colonies can be then determined.

Sugar and organic acid analysis by high-performance ionic chromatography techniques

Culture supernatant was obtained by centrifuging (MiniSpin Eppendorf, USA) fermentation broth samples in Eppendorf tubes at 13,400 rpm for 3 min and stored at −20°C. Before high-performance ionic chromatography analysis, supernatant was filtered on Minisart filters 0.2-μm pore diameter polyamide membranes (SARTORIUS, Germany) and was diluted (1:10 and/or 1:100) in deionised water. Fresh Milli-Q grade water (18.2-mΩ-cm resistance) was used for eluent preparations and sample dilutions.

Glucose and organic acids concentrations were determined using an ICS-3000 system (Dionex) equipped with an AS autosampler (Dionex) and with an ED40 electrochemical detector (amperometric and conductivity detections).

Glucose was separated on a CarboPac™ PA1 analytical (4×250 mm) and guard (4×50 mm) columns at an isocratic concentration of 25% deionised water (eluent 1) and 75% 200 mM NaOH (eluent 2), at a flow rate of 1.0 mL min^{-1} at 30°C for 15 min, followed by a pulsed amperometric detection (a working gold electrode and a reference electrode pH-Ag/AgCl combination). The waveform of pulsed amperometric detection used was: t=0.00 s, E=0.10 V; t=0.20 s, E=0.10 V (Begin); t=0.40 s, E=0.10 V (End); t=0.41 s, E=−2.00 V; t=0.42 s, E=−2.00 V; t=0.43 s, E=0.60 V; t=0.44 s, E=−0.10 V; and t=0.50 s, E=−0.10 V.

Acetate, formate, lactate, pyruvate, succinate and fumarate were separated on an IonPac AS11-HC analytical (4×250 mm) and AG11 (4×50 mm) guard columns equipped with a carbonate removal device (CRD 200, 4 mm), a continuously regenerated anion trap column and an anion self-generating suppressor (ASRS® 300, 4 mm) followed by a conductivity detection. The mobile phase was a KOH solution (EGC II KOH cartridge) at a flow rate of 1.5 mL min^{-1}. The gradient was self-generated as followed: 0 to 13 min, 1 mM KOH; 13 to 25 min, the gradient increased linearly from 1 to 15 mM KOH, raised stepwise to 30 mM from 25 to 35 min, then to 60 mM from 35 to 45 min and kept at this concentration from 45 to 50 min and finally returned to 1 mM for 20 min.

Chromatographic data were collected, analysed and quantified using Chromeleon software (version 6.80 SP4 Build 2361) and autocalibration chromatograms. External standards (glucose and organic acids) were used at the beginning, the middle and the end of sample sequence to ensure the stability along the sequence analysis. The regression coefficients were always superior to 0.99.

In situ bioluminescence measurement

Photons emitted by *E. coli yciG::luxCDABE* were counted using a photomultiplier (PMT) H7360-01 Photon Counting Head (Hamamatsu photonics K.K., Japan). PMT was connected to a glass window specifically designed in the stainless-steel lightproof bioreactor. This provides in situ light intensity detection with high efficiency through a wide effective area of lenses (22 mm diameters). Light intensity unit is relative light units (RLU) per second corresponding to the sum of the photon incidents on the PMT in 1-s integration time.

To ensure the absence of external light interferences in the bioreactor, background noise was measured and must be lower than 100 RLU s^{-1} according to the supplier's value. This very low value was neglected, regarding to an induced signal on the order of magnitude of 10^7 RLU s^{-1}.

Correction of the basal bioluminescence signal

The relative bioluminescence intensity was measured as a total intensity minus the basal level which was considered,

in our studies, to be an average of the bioluminescence intensity observed in a steady-state culture. This basal level was quite low compared with the intensity obtained from induction of the reporter gene. The relative bioluminescence intensity was then calculated according to the following equation (de Jong et al. 2010):

$$I_r(t) = I_t(t) - I_b(t)$$

where $I_t(t)$ is the total bioluminescence intensity, $I_b(t)$ is the average bioluminescence intensity during a steady-state culture, $I_r(t)$ is the relative bioluminescence intensity. Normalisation of the signal is done in order to compare different kinetics of bioluminescence responses according to the following expression:

$$I_n(t) = \frac{I_r(t)}{I_{r_{max}}(t)}$$

where $I_n(t)$ is the normalised bioluminescence intensity, $I_{r_{max}}(t)$ is the maximum value of relative bioluminescence intensity.

Gas analysis and monitoring

Inlet and exhaust gas analyses were conducted using a fermentation gas monitor system (LumaSense Technologies Europe). The system combines a multipoint sampler 1309 with a gas analyser (INNOVA 1313). The latter simultaneously measures the concentrations of oxygen (O_2) and carbon dioxide (CO_2) using two acoustic-based measurement methods: photo-acoustic spectroscopy to measure CO_2 concentrations and magneto-acoustic spectroscopy to measure O_2 concentrations. The acoustic gas analyser has excellent characteristics with regard to high precision, good accuracy, long-term stability and fast response time (0.2 s). Therefore, it is well adapted to the exhaust gas monitoring during transient responses in well-controlled high-performance bioreactors (Christensen et al. 1995).

Calculation methods

Glucose uptake and organic production rates

The glucose uptake rate (r_S), acetate and formate production rates ($r_{acetate}$ and $r_{formate}$) were calculated from their measured data by means of the respective mass balance equations, taking into account the volumetric feed medium rate and the withdrawal volume from the sampling.

Off-gas rates

The oxygen uptake rate (r_{O_2}) and carbon dioxide production rate (r_{CO_2}) were calculated from the mass balances in the gas and liquid phases as described in the Electronic supplementary material. During the substrate perturbation, exhaust gas analysis was conducted every second, considering that the composition of the inlet air maintained constant. The r_{O_2} and r_{CO_2} were calculated from the mass balance equations, taking into account the inlet and outlet gas compositions, the evolutions of the temperature, pH, salinity, liquid volume in the reactor.

Estimation of the specific growth rate during the glucose pulse

In most recent study, Taymaz-Nikerel et al. (2011) estimated the dynamics of growth rate of *E. coli* after the glucose pulse on aerobic glucose-limited chemostat by means of the degree of reduction balance and of the ATP stoichiometry (very low turnover time of ATP about 1 s). They found the same increase of growth rate estimated from these both independent calculation methods. Therefore, the changes in biomass formation rate in response to the exposure to glucose excess conditions were calculated, using the degree of reduction balance with the available measurements data (formate and acetate productions, glucose and oxygen consumptions) as mentioned in the following equation:

$$\gamma_X r_X = \gamma_S r_S + \gamma_{O_2} r_{O_2} - \gamma_{acetate} r_{acetate} - \gamma_{formate} r_{formate}$$

Then growth rates were determined as the ratio r_x/X where X is the biomass concentration.

Results

Steady-state chemostat characteristics and glucose pulse experiments

Three steady-state runs (SS1, SS2 and SS3) were characterised and assessed by a stable biomass concentration and a constant concentration of the exhaust gases. The steady-state cultures were performed at the dilution rates of 0.14 and 0.16 h^{-1}. The mean biomass yield on glucose ($Y_{x/s}$) at steady states is 0.42±0.05 $g_X g_S^{-1}$ and the mean residual glucose concentration is 0.010±0.004 mM. Trace amounts of acetate and formate were also detected in steady-state cultures, 0.06±0.01 and 0.03±0.01 mM corresponding to 0.038±0.007 and 0.021±0.007 mmol $CmolX^{-1}$ h^{-1}, respectively. The carbon and redox balances at steady-state conditions were calculated as the ratio of the amounts of carbon ($C_{substrats}/C_{products}$) and of the number of moles of electrons for transfer to O_2, corresponding to 98% and 97%, respectively (Table 1). In addition, plasmid stability of *E. coli* DPD2085 was verified throughout the chemostat. The

Table 1 Carbon and redox recoveries were calculated from the raw data of the steady state (SS) glucose-limited chemostats of *E. coli* DPD2085

Steady state	D (h^{-1})	$[S]_{feed}$ (g L^{-1})	$[X]$ ($g_X L^{-1}$)	$-q_s$	$-q_{O_2}$	q_{CO_2}	Carbon recovery (%)	Redox recovery (%)
SS1[a]	0.14	10.8	4.21±0.05	48.2±0.5	136.1±0.5	146.2±0.5	98.3±0.9	97.5±0.9
SS2[a]	0.16	11.2	4.78±0.12	52.6±2.8	136.4±8.8	147.1±8.4	98.7±2.7	98.3±2.6
SS3[a]	0.14	10.8	4.26±0.02	46.2±0.2	127.8±5.5	142.1±1.6	99.6±0.1	97.3±2.4

Average specific uptake and production rates, q_i, were expressed in mmol $CmolX^{-1}$ h^{-1} with their associated standard deviations

[a] Steady state from three independent chemostat cultures

percentage of the ratio between numbers of plasmid-bearing cells and of total cells was always superior to 80% at the moment of the glucose pulse experiments.

Table 1 represents the characterised aerobic steady states of glucose-limited chemostat runs under similar operating conditions. After at least five residence times, the glucose pulse of different intensities (0.08, 0.4 and 1 gL^{-1}) was carried out directly in the bioreactor, corresponding to time zero. The time-frame period of the glucose pulse of different intensities can be divided into three different phases (Fig. 1). Phase I, right after the glucose pulse, corresponded to the presence of excess glucose concomitant with oxygen limitation and organic acid excretion. Afterwards, phase II, *E. coli* was no longer in glucose excess conditions and the strain switched its metabolism from glucose excess to glucose limitation with a re-assimilation of acetate. Following this phase, a new glucose-limited culture was established, phase III.

Standard online measurements

Standard online measurements such as dissolved oxygen (DO), pH and volume fractions of O_2 and CO_2 in the exhaust gas reflect changes in the metabolic activity of the cells as results of modification of their environmental conditions. These parameters provide directly global observations of the cellular responses inside the bioreactor. The dynamics of these online monitoring parameters (DO, pH, off-gas O_2 and off-gas CO_2) were compared after the glucose pulse at time zero (Fig. 2). Phase I, sharp and rapid decreases in DO occurred and reached a lower level in DO between 0.4% to 2.9% (0.7 to 5.3 μmol $O_2 L^{-1}$) within about 1.5 min(Fig. 2a), thereby the cells can be considered to be under microaerobic conditions. Such a decrease of DO pointed out a rapid increase in oxygen uptake rate of *E. coli* which was consistent with the off-gas measurements (Fig. 2c, d). In the same manner, the pH values rapidly dropped due to an extracellular acidification as results of both accumulations of organic acids and produced CO_2. One can notice that the pH profile of the 0.4 gL^{-1} glucose pulse experiment was different from the two others because different proportional-integral controllers were applied for pH regulation in different experiments.

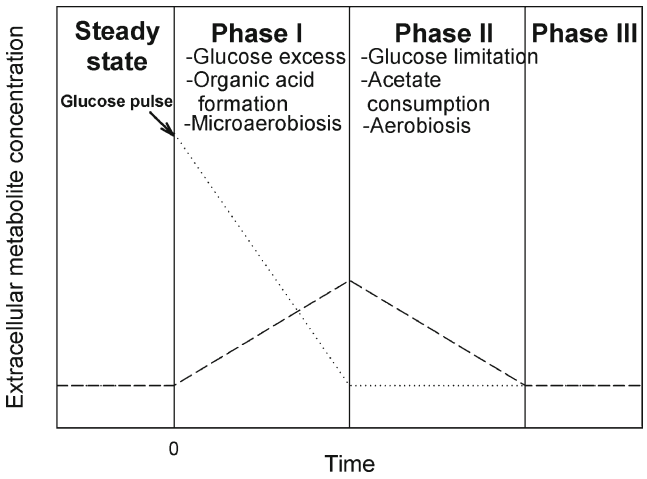

Fig. 1 Scheme of the defined different time periods after performing a glucose pulse on a steady-state chemostat culture

In phase II, the cells switched back to the glucose-limited condition, accompanied by rapid increases in DO, pH and off-gas O_2 and a gradual decrease in off-gas CO_2. Nevertheless, the dynamics in phase II were more gradual than the observed dynamics in phase I, which were due to the co-consumption of both glucose and produced acetate by *E. coli* strain during this phase.

In phase III, these online measurement parameters returned thereafter to a new pseudo-steady-state values which were slightly inferior to the previous steady-state values due to an insubstantial increase in biomass concentration.

In addition, a rapid increase in glucose concentration led to a rise in temperature inside the bioreactor (Fig. 3) and a concomitant decrease in temperature of the cooling water inside the jacket in order to maintain the temperature set-point (data not shown), indicating that the glucose pulse involved exothermic reactions. The temperature probe can then be used for the determination of the characteristic times of microbial responses due to its non-invasive and online measurement.

With standard online measurements, the similarities of these superimposed profiles were observed in response to the rapid glucose up-shift of different intensities.

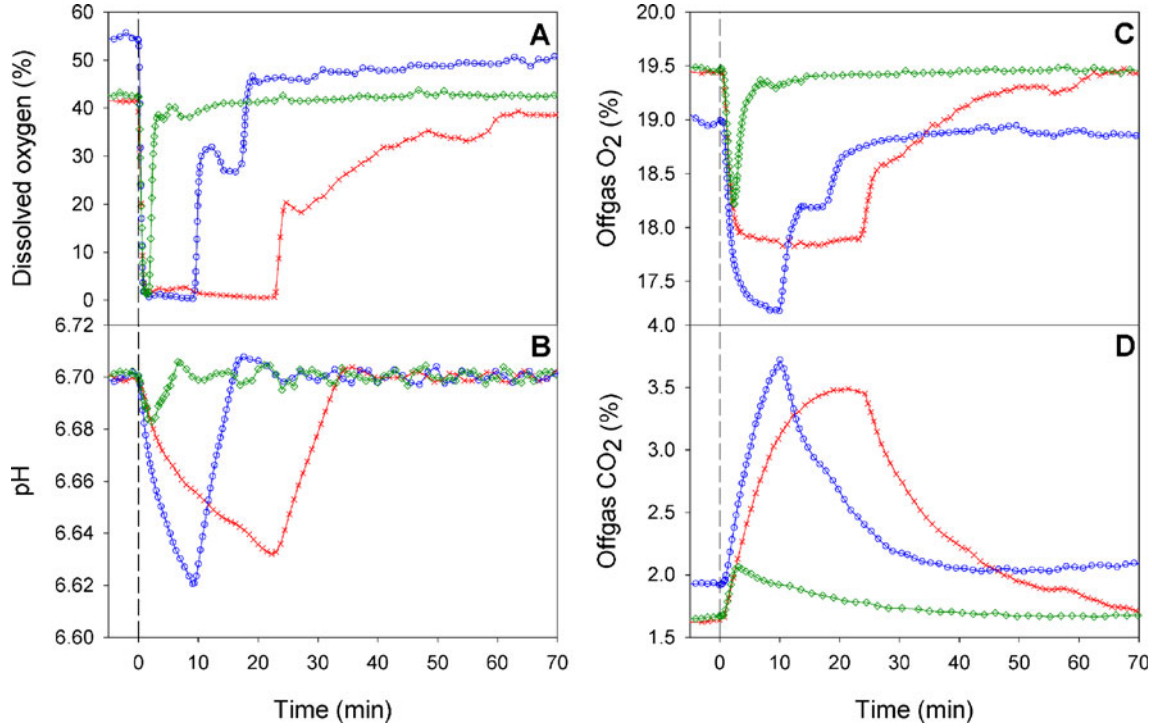

Fig. 2 Dynamics of on-line measurement parameters as results of the glucose pulses of different intensities. The measured dissolved oxygen (**a**), pH (**b**), offgas-O_2 (**c**) and off-gas CO_2 (**d**) were obtained from the glucose pulses of 0.08 gL^{-1} (*green*), 0.4 gL^{-1} (*blue*), and 1 gL^{-1} (*red*). The *symbols* indicate measured values, and the *lines* correspond to smoothed data

Transient organic acid formation and glucose consumption

In order to investigate the effect of glucose perturbations of different intensities on the dynamics of extracellular metabolite production and glucose consumption, rapid sampling with quasi-instantaneous filtration, as described in 'Materials and methods', was used to separate the supernatant from broth. Glucose and organic acid concentrations were quantified as a function of time (Fig. 4). After the glucose perturbation, the residual glucose concentration increased from the steady-state values to higher concentrations as indicated in Fig. 4a. Then the glucose was gradually consumed by *E. coli* DPD2085, describing a linear relationship with time. However, for the first 1–2 min, a progressive increase in glucose was observed that can be attributed to the micro-mixing issue inside the lab-scale bioreactor, despite the calculated mixing time at 99% of 1.55 s using a suitable correlation for the bioreactor configuration: bioreactor geometry, stirring speed (Roustan et al. 1999). This delay can be explained by the quite small size of sampling port (0.8 mm diameter) within a small time interval on the order of magnitude of seconds. This delay was verified by applying the glucose pulse in the 1 L bioreactor containing MilliQ water using the same sampling device, and a delay of quantified glucose concentration was also observed (data not shown). Such verification suggested that the observed delay was not due to the microbial activities but rather due to the sampling system and bioreactor configurations. Consequently, the period of glucose uptake for first 2 min after pulse cannot be precisely measured in these studies.

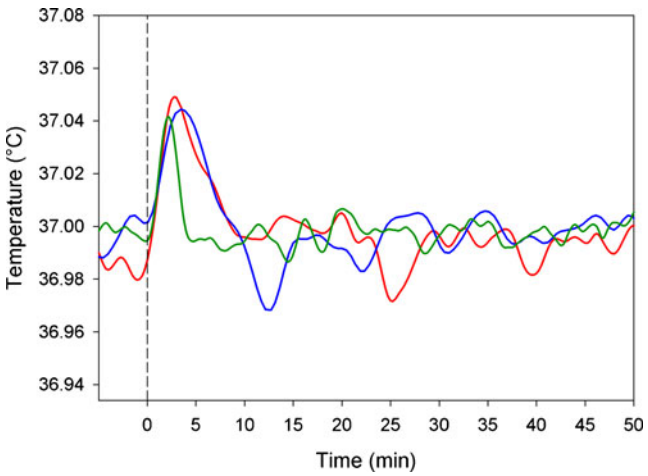

Fig. 3 Temperature evolution in response to glucose pulses: 0.08 (*green line*), 0.4 (*blue line*) and 1 gL^{-1} (*red line*)

During the transient state, the accumulations of acetate and formate were observed, whereas other organic acids and ethanol were not detected. The patterns of acetate and formate formation during the glucose perturbation of different

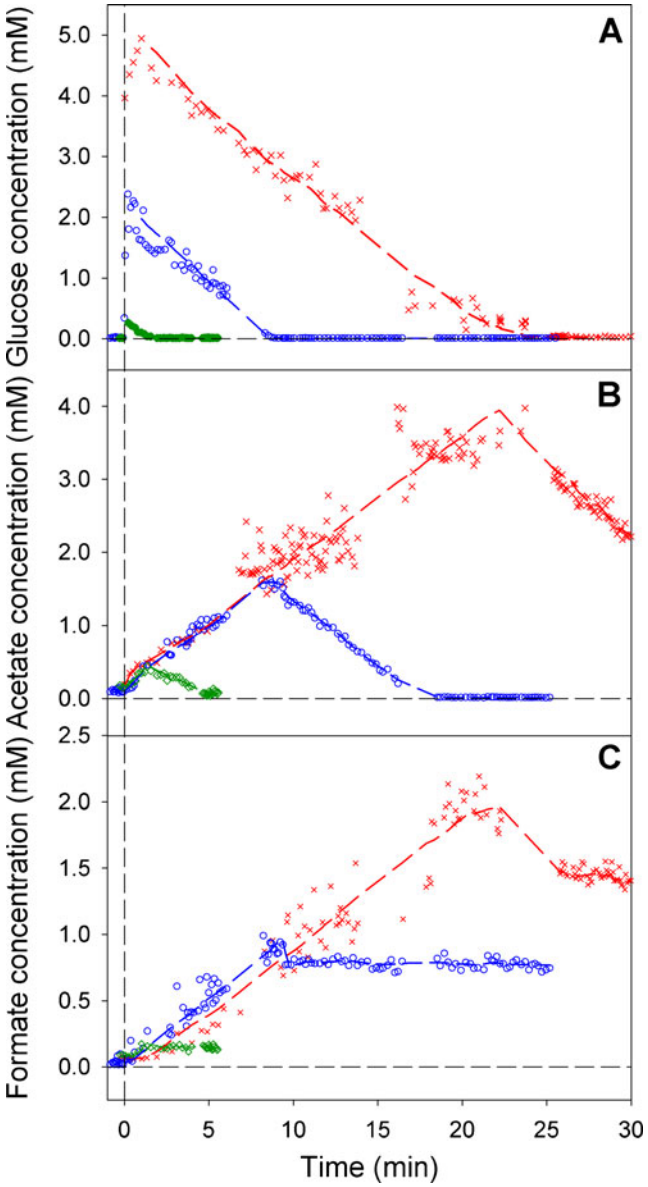

Fig. 4 Dynamic responses of residual glucose concentration and of organic acid production after the glucose pulses of different intensities: 0.08 (*green*), 0.4 (*blue*) and 1 gL^{-1} (*red*). The *symbols* indicate measured values and the *lines* correspond to smoothed data

intensities are also depicted in Fig. 4b, c, respectively. Their concentrations quasi-linearly increased in the phase I. The acetate produced in phase II was re-consumed by *E. coli* as a carbon source with a linear tendency under glucose-limited chemostat conditions. A rapid decrease in produced formate was noticed during this phase and estimated at about 22% of the maximum value, and then the residual formate concentration in the culture kept quasi-constant.

The patterns of residual glucose concentration, acetate and formate accumulations in phases I and II appeared to be similar and independent of the glucose intensities.

Dynamic responses of specific uptake and production rates

To quantify the dynamics of microbial responses to the glucose up-shifts, the specific rates of glucose consumption, acetate and formate productions ($-q_{glucose}$, $q_{acetate}$ and $q_{formate}$) were calculated from the respective mass balance equations. As described above, acetate and formate accumulations and glucose consumption followed a linear relationship as a function of time, the cells responded thus to these defined environment with their respective constant specific rates (Table 2).

The evolutions of specific oxygen uptake rate ($-q_{O_2}$) and of specific carbon dioxide production rate (q_{CO_2}) were quite reproducible in response to the independent glucose pulses in Fig. 5a, b, respectively. The initial responses for the first 8 min following the glucose pulse experiments are presented in Fig. 5c, d, respectively. The patterns of $-q_{O_2}$ and q_{CO_2} transient evolutions were similar for all experiments. The $-q_{O_2}$ and q_{CO_2} sharply increased within about 75 s to reach their maximum values and returned to quasi-stable values, independent of the glucose pulse concentrations.

The dynamics of the growth rate after the glucose perturbation were determined by means of the degree of reduction balance with the available measurement data (Fig. 6), as described in 'Materials and methods'.

Dynamic responses of whole-cell luminescent biosensor of *E. coli*

In order to have an overview of the behaviour of *E. coli* from excess glucose to glucose limitation and inversely, *E. coli* DPD2085 carrying a plasmid pDEW215 with an *yciG::luxCDABE* gene fusion was used to follow the induction of a reporter gene in response to glucose pulses of different intensities. The *yciG* gene has been reported not only to be

Table 2 Measured and calculated specific uptake and production rates of *Escherichia coli* DPD2085 in response to the glucose pulses of different intensities during phases I and II

Specific rates	Glucose pulse	Steady state	Phase I	Phase II
$-q_{glucose}$	0.08 gL^{-1}	49.0±3.3	107.9±20.5	48.8±1.8
	0.4 gL^{-1}		119.7±9.5	53.7±1.0
	1 gL^{-1}		116.0±6.1	48.1±3.8
$q_{acetate}$	0.08 gL^{-1}	0.038±0.007	62.4±16.5	−35.4±4.8
	0.4 gL^{-1}		46.8±3.6	−49.8±1.9
	1 gL^{-1}		53.5±3.1	−51.1±3.2
$q_{formate}$	0.08 gL^{-1}	0.021±0.007	20.3±10.2	–
	0.4 gL^{-1}		43.3±3.8	–
	1 gL^{-1}		32.9±2.1	–

Average uptake and production rates, q_i, were expressed in mmol $CmolX^{-1}$ h^{-1} with their associated standard deviations

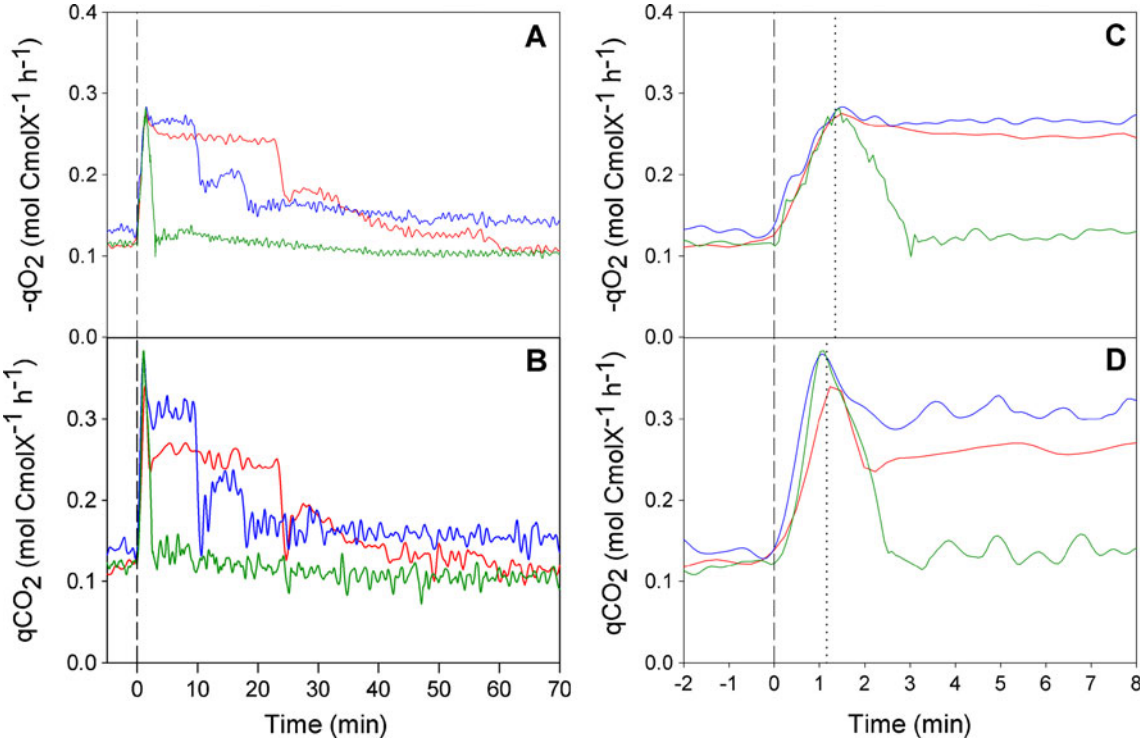

Fig. 5 Transient evolutions in the specific rates of consumed O_2 (**a**) and of excreted CO_2 (**b**). In (**c**) and (**d**), the first 8 min after the glucose pulses was being focused: 0.08 (*green line*), 0.4 (*blue line*) and 1 gL^{-1} (*red line*)

controlled under *RpoS* regulation (Kalyanaraman 2003; Rudd 2000; Weber et al. 2005) but also to be positively controlled by acidification-responsive regulatory circuits (Slonczewski and Foster 1987; Van Dyk et al. 1998; Van Dyk et al. 2004). Figure 7 represents a comparison between the dynamics of normalised bioluminescence response, specific oxygen uptake rate and the acetate formation as results of the glucose pulse of three concentrations as described above. After the glucose pulse in phase I, the bioluminescence signal sharply increased with respect to normalised bioluminescence signal within 1.5 min, accompanied by rises in acetate formation and in specific oxygen uptake rate. The transition state between the phases I and II showed an overshoot of bioluminescence signal, called a sharp peak, which occurred during the metabolic shift from the glucose excess to glucose limitation (Sunya et al. 2011). Then one can observe in phase II the bioluminescence responses obtained from the three glucose pulses were distinguished. For the 0.4 and 1 gL^{-1} glucose addition and after the glucose peak, the expressions of *yciG::luxCDABE* were observed as a bell curve. The amplitude of this belle curve was higher for the 1 gL^{-1} glucose pulse compared with the 0.4 gL^{-1} glucose pulse. This emitted light corresponded to the induction of the *yciG::luxCDABE* reporter gene in phase II for glucose pulses of 0.4 and 1 gL^{-1}, whereas it did not occur for a small pulse of 0.08 gL^{-1}. Consequently the induction of *yciG::luxCDABE E. coli* biosensor depended on the quantities of added glucose whereas other macroscopic measurements returned to a new steady state. The use of the bioluminescence strain for monitoring changes provides a direct assessment of the fluctuating effect on changes in environmental condition with in situ and online measurement, by overcoming the quenching/sampling steps compared with others available tools.

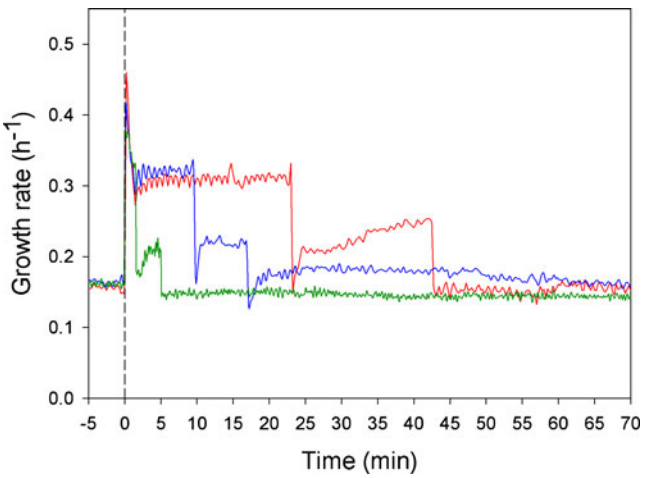

Fig. 6 Dynamics of the growth rate as results of the glucose pulses: 0.08 (*green line*), 0.4 (*blue line*) and 1 gL^{-1} (*red line*)

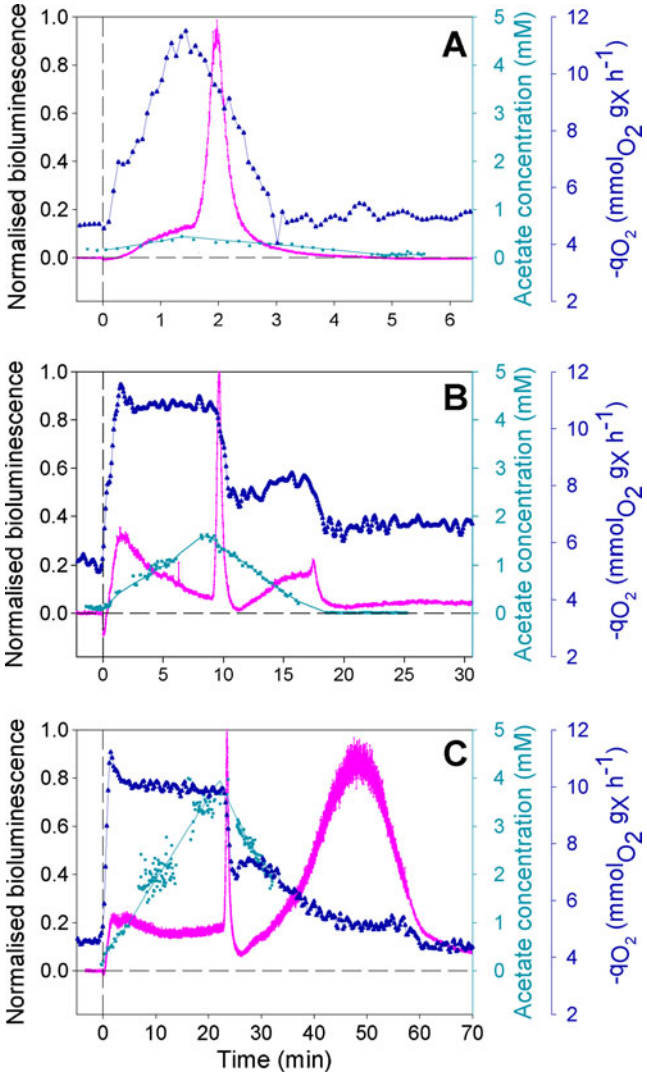

Fig. 7 In situ and online monitoring of the normalised bioluminescence responses of the *yciG::luxCDABE* reporter in comparison with the evolution in specific oxygen uptake rate and in acetate production after the glucose pulses of 0.08 (**a**), 0.4 (**b**) and of 1 gL^{-1} (**c**): *pink*, bioluminescence response; *dark cyan*, acetate production; *dark blue*, specific rate of oxygen consumption

Discussion

In large scale bioreactors, the heterogeneities due to ineffective mixing can significantly affect cell physiology and cell metabolism. Nature, intensity and frequency of gradient concentrations can be responsible for different microbial behaviour (Enfors et al. 2001; Lara et al. 2006b). Focusing on the effect of the glucose concentrations, we investigated how *E. coli* adapts its metabolism and which are its dynamics from the glucose limitation to glucose excess and inversely. An *E. coli* biosensor, plasmid-based*::luxCDABE* harbouring a stress-responsive gene, *yciG,* is used in order to in situ monitor the transcriptional induction of the promoter gene in real time.

In this study, a single glucose pulse of different intensities was performed directly in independent well-controlled steady-state cultures to monitor dynamic changes in extracellular metabolites, in the respiratory evolution as well as the growth rate in the time window of minutes. The sudden increase in available residual glucose has, in turn, engendered concomitant oxygen limitation during the glucose excess phase. Since the added glucose was depleted, the transition from glucose excess to glucose-limited conditions under aerobic conditions was also investigated. Differences in microbial behaviour on the exposure to glucose perturbations were discussed below and compared as results of three independent glucose pulses of different concentrations.

Dynamics of glucose consumption

After the glucose up-shift of different intensities to a steady-state *E. coli* DPD2085 culture, the residual glucose concentrations were linearly consumed by a first-order rate, in concordance with the previous reports (Lara et al. 2009; Link et al. 2010; Taymaz-Nikerel et al. 2011). Under these conditions, the average specific glucose uptake rates, $-q_s$ rapidly increased from 49 to 115 mmol $CmolX^{-1}$ h^{-1}, about 2.3-fold with respect to its previous steady-state value. However the $-q_s$ under glucose excess and microaerobic conditions was about 71% of the average $-q_{s,\ batch}$ in batch phase (162 mmol $CmolX^{-1}$ h^{-1}). The lower $-q_s$ compared with $-q_{s,\ batch}$ (116 vs. 276 mmol $CmolX^{-1}$ h^{-1}) were also found in the work of Taymaz-Nikerel et al. (2011). It is interesting to note that the average $-q_s$ obtained from three different concentrations of the glucose pulse approximately followed the same correlation with time, indicating that the ability of *E. coli* to uptake glucose remains unaltered in the ranges of the tested glucose concentrations (Table 2). Furthermore, the $-q_s$ sharply decreased during the phase I/phase II transitions to its former steady-state value of 50 mmol $CmolX^{-1}$ h^{-1}, despite the glucose and acetate co-metabolisation due to the re-assimilation of the produced acetate in this phase.

Dynamics of the organic acid accumulation

The trends in acetate and formate productions were nearly linear as a function of time in phase I (Fig. 4). The specific rates of acetate and formate production ($q_{acetate}$ and $q_{formate}$) were approximately constant for the three glucose pulses of different concentrations under microaerobic conditions, except for $q_{formate}$ obtained from the 0.08 gL^{-1} glucose pulse (Table 2). Consistent with these results, both acetate and formate productions were also observed as response to the glucose pulse in the works of Lara et al. (2009, 2011) and of Lin et al. (2001) where the glucose pulse was performing

outside the bioreactor. A similar glucose pulse-based experiment was carried out in a bioreactor using oxygen-enriched air in order to ensure fully aerobic conditions during the glucose excess, in that condition, acetate and formate were not detected (Taymaz-Nikerel et al. 2011). This is probably due to the low intensity of the glucose pulse (0.4 gL^{-1}) regarding to the biomass concentration (10 $g_X L^{-1}$) in the bioreactor under fully aerobic conditions.

The average $q_{acetate}$ instantaneously increased from 0.04 to 54.23 mmol $CmolX^{-1}$ h^{-1} which corresponds to the combination of the overflow and fermentative metabolisms. The accumulations of acetate and formate were clearly explained by the fact that the cells were exposed to glucose excess under oxygen-limited conditions. These results were in accordance with the simulated results of Varma et al. (1993), using flux balance approach to determine optimal microbial behaviour of *E. coli* to various levels of oxygen limitations. The authors reported that when the $-q_{O_2}$ were between 172 and 295 mmol $CmolX^{-1}$ h^{-1} (7 to 12 mmol $g_X{}^{-1}h^{-1}$) corresponding to the $-q_{O_2}$ value (250 mmol $CmolX^{-1}$ h^{-1}) obtained during phase I in this work, only acetate and formate metabolites were produced. The dissolved oxygen level has thus a strong effect on cellular metabolism, especially the metabolite production rates in order to maintain the redox balance during oxygen-limited conditions.

From previous data reported in literature, the impact of the dissolved oxygen availability on acetate accumulation was inversely correlated to the DO levels (O'Beirne and Hamer 2000; Phue and Shiloach 2005; Varma et al. 1993). The sudden increase in glucose was simulated both in aerobic and anaerobic steady-state *E. coli* cultures. Both simulations led to acetate accumulation with a specific rate higher in anaerobic conditions (97 mmol $CmolX^{-1}$ h^{-1}) compared with aerobic conditions 31 mmol $CmolX^{-1}$ h^{-1} (Lara et al. 2009). In this present study, the $q_{acetate}$ under microaerobic conditions ranges between those previous studies. However the $q_{acetate}$ dynamic patterns were different, dependent on the dissolved oxygen levels in the culture. It is interesting to note that the $q_{acetate}$ is higher, compared with $q_{formate}$ under aerobic/microaerobic conditions whereas contrary results can be observed under anaerobic conditions (Lara et al. 2009). For the three glucose pulse experiments, an immediate consumption of acetate produced was observed during the transition from phases I to II. The average specific rate of acetate consumption in phase II, $-q_{acetate}$ (45.43 mmol $CmolX^{-1}$ h^{-1}) was slightly lower compared with $q_{acetate}$ in phase I (54.23 mmol $CmolX^{-1}$ h^{-1}).

Concomitant with acetate production, formate was linearly excreted by the cells as a function of time during phase I with its specific rate of 32.17 mmol $CmolX^{-1}$ h^{-1}. In phase II, formate was no longer neither produced nor consumed. It has been reported that formate is derived from pyruvate through pyruvate formate-lyase which is activated not only under microaerobic and anaerobic conditions (Alexeeva et al. 2003) but also under aerobic conditions at a very low basal level (Pecher et al. 1982). A trace amount of formate was detected during steady-state cultures (0.021±0.007 mmol $CmolX^{-1}$ h^{-1}) and a rapid increase in formate accumulations under microaerobic conditions occurred. In phase II, formate was no longer accumulated and held nearly constant. Indeed *E. coli* genome encoded membrane-associated formate hydrogenlyase (FHL) enzyme complex which converts formate into CO_2 and H_2 (Sawers 1994). Trace amounts of selenium, molybdenum and nickel have an essential function in the formation of FHL (Ferry 1990). Without trace of selenium and Nickel in the minimum medium used in this work, the FHL was not functional; thereby no changes in residual formate concentrations occurred in phase II. Moreover Soini et al. (2008) suggested the addition of these trace elements to prevent formate accumulation which may have a toxic effect on *E. coli* cells under glucose and oxygen oscillation in lab- and large-scales bioreactors.

Dynamics of the exhaust gases

The exhaust gas monitoring of the O_2 and CO_2 content is one of the online parameter which provides a direct measurement and reflects real dynamic changes in cell respiratory activity during the environmental perturbation from seconds to minutes (Bloemen et al. 2003). The specific rates of oxygen uptake, $-q_{O_2}$, and of carbon dioxide production, q_{CO_2}, were calculated from the measured O_2 and CO_2, using the mass balance equations for the gas and liquid phases as described in Materials and methods. In phase I, the $-q_{O_2}$ and q_{CO_2}, instantaneously increased and reached their maximum values of 284 mmol O_2 $CmolX^{-1}$ h^{-1} and 376 mmol CO_2 $CmolX^{-1}$ h^{-1} within about 75 s, corresponding respectively to 71% of $-q_{O_2,max}$ (398 mmol O_2 $CmolX^{-1}$ h^{-1}) and 90% of $q_{CO_2,max}$ (417 mmol O_2 $CmolX^{-1}$ h^{-1}) in the batch phase (Fig. 5a–d). In addition, the $-q_{O_2}$ and q_{CO_2} profiles followed similar patterns for the first 75 s, independent on the glucose intensities (Fig. 5c, d). The dynamic responses of $-q_{O_2}$ and q_{CO_2} revealed an overshoot after glucose upshifts and then reached a plateau at the specific rates of 263 mmol O_2 $CmolX^{-1}$ h^{-1} and 285 mmol CO_2 $CmolX^{-1}$ h^{-1} respectively, in less than 3 min (Fig. 5c, d). Such similar overshoot of the $-q_{O_2}$ was also reported by Taymaz-Nikerel et al. (2011) where the $-q_{O_2}$ was calculated from the measured dissolved oxygen, using the dynamic dissolved oxygen balance during the pulse. These authors estimated the time required for *E. coli* to achieve a pseudo-steady state after about 60 s, faster than the results from our experiments of about 3 min. The results of this present study highlighted the fact that the *E. coli* cells rapidly consumed the dissolved oxygen before achieving a

pseudo-steady state, in response to the transition state from glucose limited to glucose excess conditions.

After the glucose pulse, one can also observe the rapid increase in CO_2 production (Fig. 2d), accompanied by a gradual decrease in pH (Fig. 2b). As it is known, the carbon dioxide exists under different forms ($CO_{2,\,gas}$; $CO_{2,\,dissolved}$; HCO_3^-; CO_3^{2-}) which are interconverted (Gutknecht et al. 1977). The equilibrium between these forms can be affected by the variation of salinity, temperature and pH of the broth. In response to the glucose up-shift, the pH decrease from 6.7 to 6.6, where HCO_3^- form is in majority (>80%) and must be taken into consideration for estimating the total CO_2 produced by the cells during the transient environmental response. The resulting dynamics of q_{CO2} profiles were quite similar to those of $-q_{O_2}$, with the overshoot for the first 3 min. We would like to highlight that the transient response of q_{CO_2} in response to pulse of glucose has not been documented in literature. Based on these results, it appears that the mechanisms of transfer of CO_2 from biomass to liquid and from liquid to gas are much more complex than a simple diffusion transfer as in the case of oxygen. Further investigation is required to elucidate the complexity of CO_2 transfers inside bioreactors.

Dynamics of the growth rate to a glucose up-shift of different concentrations

The dynamics of the calculated growth rate (μ) after the glucose up-shifts of different intensities are represented in Fig. 6. A sudden switch to glucose excess led the *E. coli* cells to instantaneous increase up to approximately 0.46 h^{-1} within 15 s, corresponding to the maximum specific growth rate ($\mu_{max,\ batch}$) observed during exponential growth in batch cultures. Then this overshoot returned to lower growth rates and reached a plateau about 0.32 h^{-1} at 90 s after the glucose pulses, estimated about 70% of the maximum growth rate, $\mu_{max,\ batch}$ (0.32 vs. 0.46 h^{-1}). This suggested that at low dilution rate (about 0.15 h^{-1}) the *E. coli* cells possessed some requisite constituents such as the enzymes involved in the metabolism but in insufficient concentrations to sustain the maximum growth rate. In the recent work of Taymaz-Nikerel et al. (2011), a strong instantaneous increase in growth rate was first reported, followed by a stable value of about 69% of the $\mu_{max,\ batch}$ (0.48 vs. 0.7 h^{-1}) within few seconds. Their finding corroborated the results from this current study. Same statement has been established by Harvey (1970), who described a brutal increase in growth rate, in RNA and proteins synthesis when addition of glucose into glucose-limited *E. coli* B-SG1 chemostat culture at low dilution rates (D<0.3 h^{-1}). Whereas, at the dilution rate greater than 0.3 h^{-1}, the exposure of glucose excess to glucose-limited culture did not cause an increase in the growth rate until after 30 to 60 min. This author found also that the cells reached its μ_{max} (0.57 h^{-1}) after two to three generation times. Moreover, Yun et al. (1996) studied the effect of the dilution rate up-shift (from 0.2 to 0.6 h^{-1}) on the variation of functional ribosome content in *E. coli* K12. After the up-shift, the functional ribosome concentration gradually increased and reached a stable concentration in 7 h. One can argue that the *E. coli* cells living at a low dilution rates contains the surplus enzymes to support the small change in substrate concentration but need a finite delay, on the time scales of hours, to be able to grow at the maximum rate.

Concerning the transition from phases I to II, the sudden decrease in growth rates was observed to rapidly reach a new pseudo-steady state. Independent on the glucose intensities, the growth rate in phase II was in average 0.21 h^{-1}, due to the co-uptake of glucose and produced acetate by the strain during this phase, leading to a higher growth rate. Interestingly, in the 1 gL^{-1} glucose pulse experiment, the specific growth rate remained nearly stable for about 6.5 min and then gradually increase from 0.21 to 0.25 h^{-1} (Fig. 6). This could indicate that *E. coli* cells need few minutes (6.5 min) to adapt its metabolism to catabolise the produced acetate more efficiently.

This work reported for the first time a comparison of the dynamics of responses of *E. coli* to glucose pulse of different intensities (0.08, 0.4 and 1 gL^{-1}) on the time scale of minutes. It was shown the ability of the *E. coli* cells to adapt their metabolism from a glucose-limited steady state to glucose excess and inversely. Despite a number of studies on microbial responses to substrate perturbation, no such comparison has been documented in the literature, under similar experimental designs (strain, medium, experimental conditions and data analysis). The following conclusions can be drawn from the present study, firstly, the *E. coli* cells can rapidly modulate, after the glucose up-shift, their specific rates of consumption ($-q_s$ and $-q_{O_2}$) and of production (q_{CO_2}, $q_{acetate}$ and $q_{formate}$) since the first seconds. However, these rates are lower (about 60% to 70%) than the maximum rates observed in batch phase. Secondly, the dynamic profiles of these responses appear to be similar and independent on the glucose pulse in the range of tested concentration. Finally, the cells are able to regain rapidly their former steady state at the macroscopic level of observation since the glucose added is depleted.

However, the monitoring of the bioluminescence signal in response to the induction of the *yciG::luxCDABE* reporter gene of *E. coli* DPD 2085 biosensor revealed on the contrary the dependence of the glucose intensities on the level of transcriptional induction of the *yciG* gene promoter (Sunya et al. 2012). The promoter *yciG* is described to be under the control of σ^s (*rpoS*) which is involved in the general stress response and strongly induced when cells enter the stationary phase (Kalyanaraman 2003; Rudd

2000; Weber et al. 2005). The *yciG* promoter is reported to be also involved in the response to cytoplasmic acidification (Van Dyk et al. 1998). Whereas the cells seem to be able to handle, at the macroscopic level, changes in substrate perturbations in the range of the tested concentrations, the cells would also activate their stress response mechanisms which could affect their long-term behaviour.

These results can be relevant to show that when the cells circulate thought the substrate fluctuations concomitant with oxygen limitation inside the large-scale bioreactors, their dynamics at the macroscopic level should be similar independently on the glucose intensities up to 1 gL^{-1}; concentrations which are in the range of Large Eddy Simulation of glucose concentration fluctuations close to the feed point in the 22 m^3 bioreactor as described by Enfors et al. (2001).

Acknowledgements The authors kindly acknowledge Dr. Tina Van Dyk, DuPont Company, USA, for the supply of the *E. coli yciG::luxCDABE* strain. Sunya S. is supported by a grant during his PhD study from Office of The Civil Service Commission, Thailand.

References

Alexeeva S, Hellingwerf KJ, de Mattos MJT (2003) Requirement of *ArcA* for redox regulation in *Escherichia coli* under microaerobic but not anaerobic or aerobic conditions. J Bacteriol 185:204–209

Bloemen HHJ, Wu L, van Gulik WM, Heijnen JJ, Verhaegen MHG (2003) Reconstruction of the O_2 uptake rate and CO_2 evolution rate on a time scale of seconds. AICHE J 49:1895–1908

Buchholz A, Hurlebaus J, Wandrey C, Takors R (2002) Metabolomics: quantification of intracellular metabolite dynamics. Biomol Eng 19:5–15

Buziol S, Bashir I, Baumeister A, Claassen W, Noisommit-Rizzi N, Mailinger W, Reuss M (2002) New bioreactor-coupled rapid stopped-flow sampling technique for measurements of metabolite dynamics on a subsecond time scale. Biotechnol Bioeng 80:632–636

Bylund F, Collet E, Enfors SO, Larsson G (1998) Substrate gradient formation in the large-scale bioreactor lowers cell yield and increases by-product formation. Bioprocess Eng 18:171–180

Chassagnole C, Noisommit-Rizzi N, Schmid JW, Mauch K, Reuss M (2002) Dynamic modeling of the central carbon metabolism of *Escherichia coli*. Biotechnol Bioeng 79:53–73

Christensen LH, Schulze U, Nielsen J, Villadsen J (1995) Acoustic off-gas analyzer for bioreactors—precision, accuracy and dynamics of detection. Chem Eng Sci 50:2601–2610

Clark DP (1989) The fermentation pathways of *Escherichia coli*. FEMS Microbiol Rev 63:223–234

de Jong H, Ranquet C, Ropers D, Pinel C, Geiselmann J (2010) Experimental and computational validation of models of fluorescent and luminescent reporter genes in bacteria. BMC Syst Biol 4:55–71

De Mey M, Taymaz-Nikerel H, Baart G, Waegeman H, Maertens J, Heijnen JJ, van Gulik WM (2010) Catching prompt metabolite dynamics in *Escherichia coli* with the BioScope at oxygen rich conditions. Metab Eng 12:477–487

Eiteman MA, Altman E (2006) Overcoming acetate in *Escherichia coli* recombinant protein fermentations. Trends In Biotechnology 24:530–536

Enfors SO, Jahic M, Rozkov A, Xu B, Hecker M, Jürgen B, Krüger E, Schweder T, Hamer G, O'Beirne D, Noisommit-Rizzi N, Reuss M, Boone L, Hewitt C, McFarlane C, Nienow A, Kovacs T, Trägardh C, Fuchs L, Revstedt J, Friberg PC, Hjertager BGBHS, Hjort S, Hoeks F, Lin H-Y, Neubauer P, van der Lans R, Luyben K, Vrabel P, Manelius A (2001) Physiological responses to mixing in large scale bioreactors. J Biotechnol 85:175–185

Ferry JG (1990) Formate dehydrogenase. FEMS Microbiol Rev 87:377–382

Gutknecht J, Bisson MA, Tosteson FC (1977) Diffusion of carbon dioxide through lipid bilayer membranes—effects of carbonic-anhydrase, bicarbonate, and unstirred layers. J Gen Physiol 69:779–794

Harvey RJ (1970) Metabolic regulation in glucose-limited chemostat cultures of *Escherichia coli*. J Bacteriol 104:698–706

Hewitt CJ, Nebe-Von Caron G, Axelsson B, McFarlane CM, Nienow AW (2000) Studies related to the scale-up of high-cell-density *E-coli* fed-batch fermentations using multiparameter flow cytometry: effect of a changing microenvironment with respect to glucose and dissolved oxygen concentration. Biotechnol Bioeng 70:381–390

Hewitt CJ, Onyeaka H, Lewis G, Taylor IW, Nienow AW (2007) A comparison of high cell density fed-batch fermentations involving both induced and non-induced recombinant *Escherichia coli* under well-mixed small-scale and simulated poorly mixed large-scale conditions. Biotechnol Bioeng 96:495–505

Hoque MA, Ushiyama H, Tomita M, Shimizu K (2005) Dynamic responses of the intracellular metabolite concentrations of the wild type and *pykA* mutant *Escherichia coli* against pulse addition of glucose or NH_3 under those limiting continuous cultures. Biochem Eng J 26:38–49

Hoque MA, Attia K, Alattas O, Merican AF (2011) Metabolic flux distribution and mathematical models for dynamic simulation of carbon metabolism in *Escherichia coli*. Afr J Biotechnol 10:2340–2352

Ishii N, Nakahigashi K, Baba T, Robert M, Soga T, Kanai A, Hirasawa T, Naba M, Hirai K, Hoque A, Ho PY, Kakazu Y, Sugawara K, Igarashi S, Harada S, Masuda T, Sugiyama N, Togashi T, Hasegawa M, Takai Y, Yugi K, Arakawa K, Iwata N, Toya Y, Nakayama Y, Nishioka T, Shimizu K, Mori H, Tomita M (2007) Multiple high-throughput analyses monitor the response of *E. coli* to perturbations. Science 316:593–597

Kalyanaraman G (2003) Construction and characterization of *yciGFE* mutants in *Escherichia coli*. Dissertation, Texas A&M University

Lara AR, Galindo E, Ramirez OT, Palomares LA (2006a) Living with heterogeneities in bioreactors. Mol Biotechnol 34:355–381

Lara AR, Leal L, Flores N, Gosset G, Bolivar F, Ramirez OT (2006b) Transcriptional and metabolic response of recombinant *Escherichia coli* to spatial dissolved oxygen tension gradients simulated in a scale-down system. Biotechnol Bioeng 93:372–385

Lara AR, Caspeta L, Gosset G, Bolivar F, Ramirez OT (2008) Utility of an *Escherichia coli* strain engineered in the substrate uptake system for improved culture performance at high glucose and cell concentrations: an alternative to fed-batch cultures. Biotechnol Bioeng 99:893–901

Lara AR, Taymaz-Nikerel H, Mashego MR, van Gulik WM, Heijnen JJ, Ramirez OT, van Winden WA (2009) Fast dynamic response of the fermentative metabolism of *Escherichia coli* to aerobic and anaerobic glucose pulses. Biotechnol Bioeng 104:1153–1161

Lin HY, Neubauer P (2000) Influence of controlled glucose oscillations on a fed-batch process of recombinant *Escherichia coli*. J Biotechnol 79:27–37

Lin HY, Mathiszik B, Xu B, Enfors SO, Neubauer P (2001) Determination of the maximum specific uptake capacities for glucose and oxygen in glucose-limited fed-batch cultivations of *Escherichia coli*. Biotechnol Bioeng 73:347–357

Link H, Anselment B, Weuster-Botz D (2010) Rapid media transition: an experimental approach for steady state analysis of metabolic pathways. Biotechnol Prog 26:1–10

Neubauer P, Junne S (2010) Scale-down simulators for metabolic analysis of large-scale bioprocesses. Curr Opin Biotechnol 21:114–121

Neubauer P, Haggstrom L, Enfors SO (1995) Influence of substrate oscillations on acetate formation and growth-yield in *Escherichia coli* glucose-limited fed-batch cultivations. Biotechnol Bioeng 47:139–146

Nienow AW (2009) Scale-up considerations based on studies at the bench scale in stirred bioreactors. J Chem Eng Jpn 42:789–796

O'Beirne D, Hamer G (2000) Oxygen availability and the growth of *Escherichia coli* W3110: a problem exacerbated by scale-up. Bioprocess Eng 23:487–494

Pecher A, Blaschkowski HP, Knappe K, Bock A (1982) Expression of pyruvate formate-lyase of *Escherichia coli* from the cloned structural gene. Arch Microbiol 132:365–371

Phue JN, Shiloach J (2005) Impact of dissolved oxygen concentration on acetate accumulation and physiology of *E coli* BL21, evaluating transcription levels of key genes at different dissolved oxygen conditions. Metab Eng 7:353–363

Roustan M, Pharamond JC, Line A (1999) Agitation Mélange Concepts théoriques de base. Technique-Ingénieur

Rudd KE (2000) EcoGene: a genome sequence database for *Escherichia coli* K12. Nucleic Acids Res 28:60–64

Sawers G (1994) The hydrogenases and formate dehydrogenases of *Escherichia coli*. Antonie Van Leeuwenhoek 66:57–88

Schaefer U, Boos W, Takors R, Weuster-Botz D (1999) Automated sampling device for monitoring intracellular metabolite dynamics. Anal Biochem 270:88–96

Schaub J, Reuss M (2008) In vivo dynamics of glycolysis in *Escherichia coli* shows need for growth-rate dependent metabolome analysis. Biotechnol Prog 24:1402–1407

Slonczewski JL, Foster JW (1987) pH-regulated genes and survival at extreme pH. In: Neidhardt FC (ed) *Escherichia coli* and *Salmonella typhimurium*: cellular and molecular biology. American Society for Microbiology, Washington, DC, pp 1539–1549

Soini J, Ukkonen K, Neubauer P (2008) High cell density media for *Escherichia coli* are generally designed for aerobic cultivations—consequences for large-scale bioprocesses and shake flask cultures. Microb Cell Fact 7:26

Sunya S, Gorret N, Delvigne F, Uribelarrea JL, Molina-Jouve C (2012) Real-time monitoring of metabolic shift and transcriptional induction of *yciG:luxCDABE E. coli* reporter strain to a glucose pulse of different concentrations. J Biotechnol 157:379–390

Taymaz-Nikerel H, van Gulik WM, Heijnen JJ (2011) *Escherichia coli* responds with a rapid and large change in growth rate upon a shift from glucose-limited to glucose-excess conditions. Metab Eng 13:307–318

Theobald U, Mailinger W, Reuss M, Rizzi M (1993) In vivo analysis of glucose-induced fast changes in yeast adenine-nucleotide pool applying a rapid sampling technique. Anal Biochem 214:31–37

Van Dyk TK, Rosson RA (1998) *Photorhabdus luminescens luxCDABE* promoter probe vectors. Methods in Molecular Biology 102:85–95

Van Dyk TK, Ayers BL, Morgan RW, Larossa RA (1998) Constricted flux through the branched-chain amino acid biosynthetic enzyme acetolactate synthase triggers elevated expression of genes regulated by *rpoS* and internal acidification. J Bacteriol 180:785–792

Van Dyk TK, DeRose EJ, Gonye GE (2001a) LuxArray, a high-density, genomewide transcription analysis of *Escherichia coli* using bioluminescent reporter strains. J Bacteriol 183:5496–5505

Van Dyk TK, Wei Y, Hanafey MK, Dolan M, Reeve MJG, Rafalski JA, Rothman-Denes LB, LaRossa RA (2001b) A genomic approach to gene fusion technology. Proc Natl Acad Sci U S A 98:2555–2560

Van Dyk TK, Templeton LJ, Cantera KA, Sharpe PL, Sariaslani FS (2004) Characterization of the *Escherichia coli AaeAB* efflux pump: a metabolic relief valve? J Bacteriol 186:7196–7204

Varma A, Boesch BW, Palsson BO (1993) Stoichiometric interpretation of *Escherichia coli* glucose catabolism under various oxygenation rates. Appl Environ Microbiol 59:2465–2473

Visser D, van Zuylen GA, van Dam JC, Eman MR, Proll A, Ras C, Wu L, van Gulik WM, Heijnen JJ (2004) Analysis of in vivo kinetics of glycolysis in aerobic *Saccharomyces cerevisiae* by application of glucose and ethanol pulses. Biotechnol Bioeng 88:157–167

Weber H, Polen T, Heuveling J, Wendisch VF, Hengge R (2005) Genome-wide analysis of the general stress response network in *Escherichia coli*: sigma(S)-dependent genes, promoters, and sigma factor selectivity. J Bacteriol 187:1591–1603

Wolfe AJ (2005) The acetate switch. Microbiol Mol Biol Rev 69:12–50

Xu B, Jahic M, Blomsten G, Enfors SO (1999) Glucose overflow metabolism and mixed-acid fermentation in aerobic large-scale fed-batch processes with *Escherichia coli*. Appl Microbiol Biotechnol 51:564–571

Yun HS, Hong J, Lim HC (1996) Regulation of ribosome synthesis in *Escherichia coli*: effects of temperature and dilution rate changes. Biotechnol Bioeng 52:615–624

Zanzotto A, Boccazzi P, Gorret N, Van Dyk TK, Sinskey AJ, Jensen KF (2006) In situ measurement of bioluminescence and fluorescence in an integrated microbioreactor. Biotechnol Bioeng 93:40–47